Biosensors and Bioelectronics 137 (2019) 199–206

Contents lists available at ScienceDirect

Biosensors and Bioelectronics

journal homepage: www.elsevier.com/locate/bios

Low-cost and user-friendly biosensor to test the integrity of mRNA molecules suitable for field applications

Ignacio Moya Ramírez[a,b], Cleo Kontoravdi[a,b], Karen M. Polizzi[a,b,*]

[a] Department of Chemical Engineering, Imperial College London, London, SW7 2AZ, United Kingdom
[b] Imperial College Centre for Synthetic Biology, Imperial College London, London, SW7 2AZ, United Kingdom

ARTICLE INFO

Keywords:
RNA integrity
Biosensor
Low-cost
Low-tech
Point-of-care diagnostics
RNA degradation

ABSTRACT

The use of mRNA in biotechnology has expanded with novel applications such as vaccines and therapeutic mRNA delivery recently demonstrated. For mRNA to be used in patients, quality control assays will need to be routinely established. Currently, there is a gap between the highly sophisticated RNA integrity tests available and broader application of mRNA-based products by non-specialist users, e.g. in mass vaccination campaigns. Therefore, the aim of this work was to develop a low-cost biosensor able to test the integrity of a mRNA molecule with low technological requirements and easy end-user application. The biosensor is based on a bi-functional fusion protein, composed by the λN peptide that recognizes its cognate aptamer encoded on the 5' end of the RNA under study and β-lactamase, which is able to produce a colorimetric response through a simple test. We propose two different mechanisms for signal processing adapted to two levels of technological sophistication, one based on spectrophotometric measurements and other on visual inspection. We show that the proposed λN-βLac chimeric protein specifically targets its cognate RNA aptamer, boxB, using both gel shift and biolayer interferometry assays. More importantly, the results presented confirm the biosensor performs reliably, with a wide dynamic range and a proportional response at different percentages of full-length RNA, even when gene-sized mRNAs were used. Thus, the features of the proposed biosensor would allow to end-users of products such as mRNA vaccines to test the integrity of the product before its application in a low-cost fashion, enabling a more reliable application of these products.

1. Introduction

The exceptional growth in the understanding and ability to manipulate and control biological processes is shaping a number of diverse fields such as medicine, the pharmaceutical and chemical industries and agriculture (Carlson, 2016; Morrison and Lähteenmäki, 2018; Philp, 2018). A clear example is the emergence of RNA vaccines, which offer flexibility to produce a wide range of antigens within a short period of time and at a low cost, because of their ease of production and the low infrastructure costs (Kis et al., 2019).

Mastery of new biological techniques and the development of new bioproducts is driving a parallel innovation in the collection of data and control over processes. Currently there is a broad range of sensors and instruments capable of measuring a wide variety of inputs, ranging from physical conditions to proteins and metabolites, either *in vitro* or *in vivo*. From high-throughput systems able to collect a huge amount of information to miniaturized sensors that specifically target a molecule and require minimal resources, there is a large number of available techniques that fit diverse purposes such as the study of biosystem dynamics, disease detection or quality control during manufacturing (Constantinou and Polizzi, 2013; Zhang et al., 2013). Among them, biosensors and bio-inspired signalling systems offer outstanding diversity and selectivity towards the target analyte and are suitable, for example, for scaling down to the single molecule detection level (Hall et al., 2016; Polizzi and Kontoravdi, 2015). Their versatility and robust performance make biosensors applicable in many different fields such as disease diagnosis and medicine, drug development and manufacture, protein biology or environmental monitoring (Vigneshvar et al., 2016). Likewise, scientific interest in the field of biosensors and detection/quantification systems is focused on improving their sensitivity and reliability, decreasing the limit of detection and response time, making them compatible with multiplexing, regenerable, portable or more cost efficient for instance (Choi et al., 2017; Vigneshvar et al., 2016).

RNAs are cornerstone molecules in biology, relevant in a wide diversity of processes. For this reason, there are optimized and commercially available techniques for their detection, characterization and

* Corresponding author. Department of Chemical Engineering, Imperial College London, London, SW7 2AZ, United Kingdom.
E-mail address: k.polizzi@imperial.ac.uk (K.M. Polizzi).

https://doi.org/10.1016/j.bios.2019.05.008
Received 29 January 2019; Received in revised form 17 April 2019; Accepted 3 May 2019
Available online 07 May 2019
0956-5663/

quantification, which range from the very simple to the highly complex. UV spectrophotometry is the simplest and most cost-effective standard alternative, offering a high sensitivity and rapid response. However, it is unable to detect integrity, a feature that is crucially relevant for easily degradable molecules such as RNA. Microfluidic electrophoresis is the most established, accurate and high-throughput technique to determine RNA integrity to date. However, this approach has some limitations such as the need for specialized equipment and expensive consumables, as well as lack of sensitivity to small alterations in the RNA (e.g. loss of a few nucleotides) and loss of accuracy for big molecules (usually above 6 kb). Reverse transcription PCR (RT-PCR) is another alternative, which can go beyond quantification. For example Blewett et al. (2011) developed a splinted ligation and quantitative reverse transcription polymerase chain reaction (qSL-RT-PCR) assay capable of differentiating between capped and uncapped mRNA. In addition, through cDNA synthesis it is possible to reach the level of single-cell RNA sequencing (La Manno et al., 2018; Strobel et al., 2018). RT-based systems, though, require extensive optimization and depend on a number of factors such as primer design, the reverse transcriptase used or DNA contamination.

Other biosensors based on electrochemical or optical transducers in conjunction with biomolecular recognition have been used for RNA detection and characterization. For example, Fang et al. proposed a label-free biosensor based on surface plasmon resonance (SPR) to detect miRNAs at concentrations lower than 10 fM (Fang et al., 2006). Carrascosa et al. (2012) also used SPR to detect RNA upon the formation of a triplex with a DNA probe. Tedeschi et al. (2005) developed a reusable microgravimetric biosensor equipped with an oligonucleotide probe able to quantify RNA concentrations in the nM range. Finally, Halford et al. (2013) developed an electrochemical sensor targeting 16sRNA for bacterial detection and quantification.

Overall, most of the existing RNA biosensors are based on complementary oligonucleotide probes (Carrascosa et al., 2016). However, a common characteristic of all these alternatives is their high technological requirements, which makes them unsuitable for field-based applications or non-specialist end-users. Within this context, the aim of this work was to develop a mRNA biosensor combining the simplicity of spectrophotometric measurements with the ability to detect molecular integrity. Our research is motivated by the promising development of mRNA vaccines as prophylactic alternatives (Pardi et al., 2018), since a system enabling direct RNA integrity tests by the end-user in the field before the mRNA vaccine is administered will be of great applicability. The proposed biosensor would address the need for compatible point-of-care technologies (Hu et al., 2014), and thus would be applicable, for instance, in vaccination campaigns with a limited availability of specialized technology. Furthermore, the proposed sensor, without any further modification, would also be suitable for more sophisticated and accurate integrity tests, that could be used for industrial quality control of RNA vaccines.

The key component of the sensor is a bi-functional protein with RNA biorecognition and reporting properties, namely, a fusion protein between the λN domain of the λ phage and a β-lactamase (λN-βLac). The strong and specific interaction between the λN peptide and its cognate boxB hairpin has been demonstrated previously (K_d in the range of 1–2 nM) (Qi et al., 2010; Zhang et al., 2010). In Nature, λN peptide acts as a transcription antitermination agent in its natural host, *E. coli*., via recognition of its cognate boxB aptamer (Mishra et al., 2013; Santangelo and Artsimovitch, 2011). The interaction is highly specific. Indeed, studies analysing the effect of single base pair substitutions on the interaction show that small changes lead to a decrease in strength of the binding (Kawakami et al., 2006; Tan and Frankel, 1995). Moreover, the λN – boxB system has been used for *in vivo* RNA visualization by inserting several repeats of the aptamer upstream of the target gene (Daigle and Ellenberg, 2007; Martin et al., 2013). The signal-to-noise ratio reported in these studies suggests that λN does not recognise any random sequences within the *E. coli* transcriptome. In addition to the high affinity of their interaction, the interest in the λN/boxB hairpin pair stems from their considerably small size (Lampasona and Czaplinski, 2016), which leads to minimal disruption of the RNA to be studied. The λN peptide has 22 amino acids; thus it is easy to fuse to other protein and express. It is also able to interact with its cognate aptamer strongly and specifically (García-García and Draper, 2003; Ke et al., 2012). Indeed, the tandem λN peptide/boxB RNA motif has already been used for RNA purification (Di Tomasso et al., 2011). The fusion protein designed as the key part of the biosensor, λN-βLac, incorporates this peptide as the mRNA recognition element.

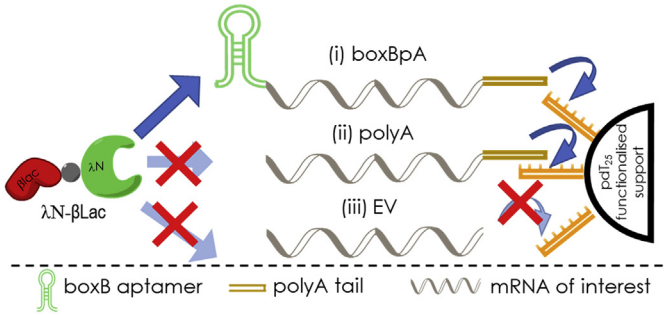

Fig. 1. Biosensor design. Three **model mRNA molecules** are depicted: (i) **boxBpA** full-length mRNA, that has a boxB aptamer at the 5′-end and a polyA tail at the 3′-end; (ii) **polyA** RNA without the boxB aptamer, thus simulating a 5′ degradation and (iii) **EV** RNA that lacks both the boxB aptamer and the polyA tail. Both the boxBpA and polyA RNAs will hybridize with the pdT_{25} oligos on the solid support, however only boxBpA will be recognized by the fusion protein λN-βLac. The biosensor will only produce a signal if both binding events take place, *i.e.*, only if the RNA is immobilized on the beads and λN-βLac binds to the RNA. Otherwise, either the RNA will be washed out of the system or the protein will not bind to it. In both cases the reporter protein λN-βLac will not be present during the colorimetric assay, and a signal will not be generated.

The biosensor proposed in this work is based on two binding events that will only take place if the RNA molecule is intact, as depicted in Fig. 1. First, the RNA molecule must be immobilized on poly-deoxythymidine (pdT_{25}) oligonucleotide-coated beads through its 3′-end poly A tail. Afterwards, the λN domain from the λN-βLac fusion protein will specifically recognize its cognate aptamer (the boxB motif) encoded in the 5′-end of the molecule and bind to the immobilized RNA. The β-lactamase enzyme of the fusion protein can then be used as reporter of the molecular integrity of the RNA molecule by means of a simple colorimetric assay that can be analyzed by a spectrophotometer or interpreted by visual inspection. If RNA degradation occurs, either one or both binding events will not take place; thus blocking the response of the biosensor.

2. Materials and methods

2.1. Chemicals

General use chemicals such as culture media, β-D-1-thiogalactopyranoside (IPTG), salts and buffers were analytical grade and purchased from Sigma Aldrich (UK). Oligonucleotides were synthetized by Invitrogen (US), and nitrocefin was purchased from Thermo Fisher Scientific (UK).

2.2. Plasmid construction

All the constructs were based on the plasmid pET-28a (+) (Novagen, UK). The primers used are indicated Table S1. *E. coli* DH5α (New England Biolabs, NEB, UK) was used as a cloning strain. To generate pET28a-λN-βLac the RNA binding peptide λN was PCR-amplified using Phusion DNA polymerase (NEB) with primers 1 and 2 from the plasmid pET42a-λN + -L + -GSH (Di Tomasso et al., 2011),

purchased form Addgene (US), plasmid number # 98894. A Gly-Ala_{x10} linker was introduced in the 5' end of the reverse primer. The AmpR gene, encoding the β-lactamase, was amplified from the plasmid pET-15b using primers 3 and 4, excluding the signal peptide from the amplified sequence. Both parts were inserted into the pET-28a (+) vector upstream the C-terminal His tag, amplified with primers 5 and 6, via Gibson DNA assembly (Gibson et al., 2009). The pET28a-βLac control plasmid was assembled in a similar way, amplifying the AmpR gene with primers 4 and 7, and pET-28a (+) with primers 8 and 9.

DNA constructs for the synthesis of RNA molecules were prepared as follows. To generate pET28a-polA, the plasmid pET-28a (+) was digested with *Not*I and *Xho*I (NEB), gel purified and ligated with a 50 nt polyA DNA fragment flanked with the correspondent restriction sites that was previously generated by annealing of the oligos polyA-F and polyA-R (Table S2) using T4 ligase (Promega, UK). The product of the ligation was transformed into *E. coli*. Similarly, pET28a-B-polA was digested with *Xba*I and *Nde*I and ligated with a DNA fragment encoding the boxB aptamer obtained by annealing the oligos boxB-F and boxb-R (Table S2), generating pET28a-B-polA. For the construction of the longer RNA templates, an 815 bp section of the *lacI* gene was amplified with the primers 12 and 13 and inserted into pET28a-B-polA and pET28a-polA previously amplified with primers 14 and 15 to generate the plasmids pET28a-B-polA-lac and pET28a-polA-lac, respectively.

All the constructs were verified by sequencing prior to further use (Eurofins Genomics, Ebersberg, Germany).

2.3. In vitro transcription of RNA molecules

Three model RNA molecules: EV (empty vector, lacking both the polyA and boxB), polA, and boxBpA, and the two longer mRNA pA-lac and boxBpA-lac were synthetized by *in vitro* transcription using the DNA templates obtained by PCR-amplification of the plasmids pET-28a, pET28a-polA, pET28a-B-polA pET28a-polA-lac and pET28a-B-polA-lac respectively, with primers 10 and 11. The product of the PCR reaction was linearized with *Xho*I and gel-purified.

In vitro transcription reactions were run in a total volume of 150 µL containing 40 µL of DNA template (1–1.5 µg), 90 U of T7 RNA polymerase (Thermo), 0.75 µL of each 100 mM NTPs, 30 µL of 5X transcription buffer (Thermo), and 60 U of RNase inhibitor (NEB). The reaction was incubated at 37 °C for 4 h. Subsequently, the DNA template was digested with 3.75 µL DNase I (NEB) for 1 h at 37 °C. Finally, the RNA was purified with the Clean & Concentrator kit (Zymo Research, UK), eluted with RNase free water, aliquoted and stored at −80 °C.

2.3.1. RNA refolding

Prior to use, the RNA was refolded to recover its tertiary structure, adapting the protocol suggested by Cantara et al. (2017). Initially an aliquot of purified RNA was defrosted on ice. The RNA concentration was adjusted using RNase free water and Buffer A to a final composition of 50 mM HEPES, 78.7 mM NaCl, pH 7.4, supplemented with 0.4 U/µL of RNase inhibitor. The mixture was incubated at 80 °C for 2 min, followed by 60 °C for 2 min. Finally, 50 mM $MgCl_2$ was added to a final concentration of 1 mM followed by a final incubation at 37 °C for 30 min.

2.4. Protein expression and purification

The plasmids pET28a-λN-βLac and pET28a-βLac were transformed into *E. coli* BL21 (DE3) competent cells (NEB) to express the λN-βLac and βLac proteins, respectively. An inoculum culture was grown overnight at 30 °C and 250 r.p.m. in lysogeny broth (LB) medium containing 50 µg/mL of kanamycin. Subsequently, 50 mL of medium was inoculated with 1.25% v/v of the inoculum culture. Cells were grown at 30 °C and 250 r.p.m. until an OD_{600} of 0.5 and the protein expression was induced with IPTG to a final concentration of 0.5 mM. After 16 h of culture at 25 °C, cells were pelleted by centrifugation at 4 °C for 10 min at 4000 × *g* and resuspended in 5 mL of resuspension buffer (50 mM NaH_2PO_4, 600 mM NaCl, 5 mM imidazole, 5% glycerol, pH 8). The suspension was supplemented with 1 mM PMSF and 1 mg/mL of lysozyme (final concentrations) and incubated for 30 min at 4 °C. Cells were disrupted by sonication for 3 min (10 s ON/OFF cycles, 75% amplitude) at 4 °C with a Vibra Cell (Sonics, UK) sonicator equipped with a one-quarter inch probe. The insoluble fraction was pelleted by centrifugation at 16,000 × *g* for 30 min at 4 °C. The soluble fraction was incubated with 1 mL of 50% Ni-NTA agarose resin (Qiagen, UK) for 1 h at 4 °C with gentle agitation. The resin was washed twice with 4 mL of wash buffer (50 mM NaH_2PO_4, 600 mM NaCl, 50 mM imidazole, 5% glycerol, pH 8). Finally, the protein was recovered in 4 elution fractions of 0.5 mL with elution buffer (50 mM NaH_2PO_4, 600 mM NaCl, 250 mM imidazole, 5% glycerol, pH 8). The third and fourth fractions were combined and buffered-exchanged using centrifugal column concentration with a 5 kDa MWCO (Vivaspin 2, GE Healthcare, UK). One mL of conservation buffer (HEPES 50 mM, NaCl 130 mM, EDTA 0.5 mM, 5% v/v glycerol and pH 7.4) was run through the column three times, and the final volume reduced to 200 µL.

2.5. Gel shift assays

Each RNA-protein binding assay took place in a final volume of 8 µL, where 5 pmol of RNA was incubated with the protein, either λN-βLac or βLac, at molar ratio of 1:2 RNA:protein in buffer A (50 mM HEPES, 78.7 mM NaCl, RNase inhibitor 160 U/mL, pH 7.4) for 1 h at room temperature. The whole reaction was loaded in a TGX™ (Bio-Rad, UK) gel and electrophoresed in 0.5xTBE buffer at 20 mA and 4 °C for 30 min. The RNA was visualized with SYBRsafe (Thermo).

2.6. Biolayer interferometry experiments

Biolayer interferometry (BLI) experiments were performed with a BLItz® (ForteBio, US) interferometer equipped with high precision streptavidin (SAX, ForteBio) sensors. Prior to use, the sensors were hydrated with buffer A for at least 10 min and kept submerged in the buffer until being inserted in the instrument for a maximum of 1 h.

The BLI assays were performed in a series of steps: (i) an initial equilibration step for 30 s with 250 µL of buffer A; (ii) binding of biotinylated pdT_{25} oligonucleotide using 250 µL of a 0.1 µM solution in buffer A for 1 min; (iii) wash with 250 µL of buffer A for 30 s; (iv) binding of the refolded RNA using 4 µL of 2 µM RNA for 5 min; (v) wash with 250 µL of buffer B (50 mM HEPES, 200 mM NaCl, 0.1% BSA, 0.02% Tween 20, pH 7.4) for 30 s; (vi) protein binding with 250 µL of 0.70 µM λN-βLac or βLac in buffer B for 10 min; (vii) desorption with 250 µL of buffer B for 2 min. Buffer A was modified to buffer B when the protein was present in the assay in order to minimize the non-specific binding between RNA and protein. All the experiments were run in triplicate.

2.7. Biosensor assays

The biosensor assays were performed as follows: (*i*) 10 µL of streptavidin-coated magnetic beads 1% w/v (Dynabeads C1, Thermo) were washed three times with 200 µL of buffer A; (ii) 50 µL of a 0.2 µM solution of pdT_{25} in buffer A during 10 min was bound to the beads; (iii) the beads were washed with 200 µL of buffer A; (iv) 20 µL of 0.6 µM RNA in buffer A was allowed to bind for 20 min; (v) the beads were washed with 200 µL of buffer B; (vi) 50 µL of 0.3 µM protein solution was added for 1 h; (vii) the beads were washed with 200 µL of buffer B three times; (viii) the beads were resuspended in 100 µL of buffer B. All the binding steps took place at room temperature and 700 r.p.m. 4 µL of the resuspended beads (equivalent to 4 µg of beads) were added to 190 µL of nitrocefin reaction mix (0.1 mM nitrocefin, 50 mM phosphate buffer pH 7) and the absorbance at 492 nm was measured in a POLARsar Omega (BMG Labtech, UK) plate reader for 1 h. For the

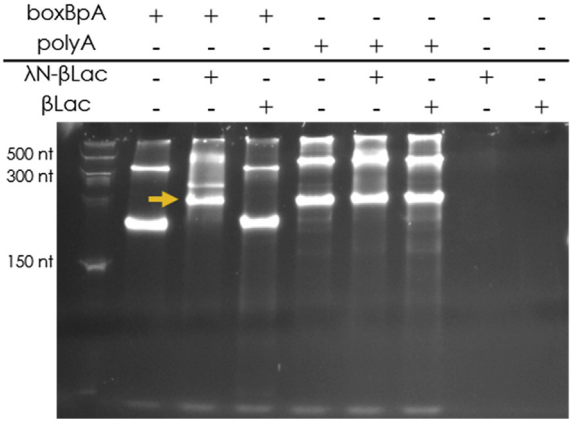

Fig. 2. Gel shift assay. Two different model RNAs, boxBpA and polyA, were combined with λN-βLac or βLac and loaded on a native TGX gel. Controls with only boxBpA, polyA, λN-βLac or βLac were also included (lanes 1, 4, 7 and 8 respectively). A slower migration pattern was observed only when both boxBpA and λN-βLac were present (lane 2, yellow arrow), suggesting an interaction between them. Ladder: low range ssRNA (NEB). (For interpretation of the references to color in this figure legend, the reader is referred to the Web version of this article.)

experiment with gene-length mRNAs the assay was slightly modified, to increase the dynamic range of the sensor. The pdT_{25} concentration was increased to 5 μM and the λN-βLac concentration increased to 0.6 μM, using 8 μg of beads in the colorimetric test.

3. Results and discussion

3.1. Gel shift analyses

Gel shift analyses were used as a preliminary source of information about the interaction between λN-βLac and the RNA at different integrity states. Native gel electrophoresis analysis was used to preserve the interaction between the RNA and the protein during the analysis.

The gel shift experiment confirms that the λN-βLac fusion protein specifically binds to the RNA containing the boxB aptamer (RNA boxBpA), as shown in Fig. 2, lanes 1 to 3. RNA boxBpA migrates the same distance in the absence of protein or when βLac (control protein not fused to λN) is added. However, when λN-βLac is used instead, RNA boxBpA migration through the gel was slower, suggesting an interaction between the protein and the RNA. The same experiments were reproduced using a control RNA lacking the boxB aptamer (polyA RNA, lanes 4 to 6, representing cleavage or degradation of the 5' end). In this case the RNA migrated similarly in all three cases, regardless of the presence of protein or identity of the protein used, which confirms that there are no non-specific interactions between either of the two proteins and the rest of the RNA molecule in the absence of the aptamer.

The presence of multiple RNA bands in all lanes of the gel could be due to different RNA secondary structures or dimerization of the model RNAs. When the samples are run on a denaturing urea gel, the additional bands disappear almost completely (data not shown), providing further evidence in support of this hypothesis.

The results provide preliminary evidence that the λN-boxB interaction functions appropriately for use in the biosensor. However, the gel shift assay does not reproduce the exact conditions that would be used for the biosensor operation in terms of buffering conditions and the sequence of molecular capture or binding.

3.2. Biolayer interferometry analysis

To fully characterize the system, biolayer interferometry analyses were used, since this enabled the study of each step necessary for the

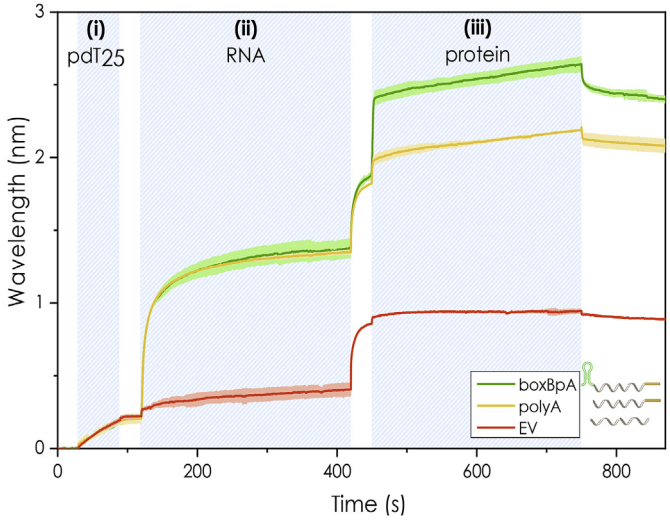

Fig. 3. Biolayer interferometry tests. Three different RNA molecules are assayed: a model full-length RNA molecule with a boxB aptamer at the 5′-end and a polyA tail at the 3' (boxBpA); a RNA lacking the boxB aptamer, thus simulating a RNA degraded from the 5'end (polyA) and a RNA without both the aptamer and the polyA tail (EV) simulating a RNA further degraded on its 3′ end. The shaded areas correspond to the **binding events** taking place: (i) loading of the biotinylated polydT25; (ii) **RNA binding**, and (iii) **protein binding** (λN-βLac). A final desorption step is included in the assay. The intermediate steps in between the binding ones correspond to washing and equilibration steps (see material and methods section). The average value (line) and SD (shaded) for three replicate experiments are shown. No interaction between EV, lacking a polyA tail, and the $polydT_{25}$ oligo occurs. Moreover, λN-βLac only recognizes the boxBpA RNA, specifically binding to it during the step (iii). Whereas in the other two cases, the protein-RNA interaction is negligible.

biosensor function (in terms of both kinetics and intensity). Therefore, this technique allowed us to optimize the buffer conditions to minimize non-specific binding between DNAs, RNAs and/or proteins. The results displayed in Fig. 3 correspond to experiments carried out with three different model RNA molecules: full-length RNA molecule carrying a boxB aptamer in the 5′ end and a polyA tail in the 3' (boxBpA); a RNA simulating 5′-degradation, which lacks the nucleotides of the boxB aptamer (polyA), and a RNA without both ends, therefore simulating a molecule further degraded on its 3′ end (EV).

All three expected binding events were detected, *i.e.*, the loading of the $polydT_{25}$ oligo on the beads, immobilization of the RNA by interactions between the $polydT_{25}$ oligo and the polyA tail of the RNA, and λN-βLac binding to the RNA through its boxB aptamer (marked as shaded regions in Fig. 3). In addition, the results show that the λN peptide, once fused to the N-terminus of βLac to form the λN-βLac fusion protein, satisfactorily retains its affinity and selectivity towards the boxB aptamer (boxBpA RNA), while it does not bind to the RNA molecules when the cognate hairpin is missing (polyA and EV RNAs). The loading of the sensor with the biotinylated $polydT_{25}$ oligo takes place initially, reaching a signal of approximately 0.18 nm after 1 min of binding. Subsequently, after a 30 s step for baseline stabilization with buffer A, the RNA samples are loaded into the interferometer. At this stage, binding of the RNA only takes place when using polyA and boxBpA RNAs, for which the signal increases up to 1.3 nm, and not for EV. Therefore, as expected, there is no interaction between RNA lacking a polyA tail and the $polydT_{25}$ oligo. After that, another washing step is conducted, using buffer B. The increase in the signal detected during this second wash step is due to the change in the salt content and the presence of new components (*i.e.* BSA and Tween 20) in buffer B compared to buffer A, with no additional binding events. During the third and last binding step, λN-βLac only binds to the sensor in the experiments where boxBpA RNA had been previously used. In the other

two cases, the protein does not interact with the DNA oligos when EV RNA is used, and its interaction with the RNA is negligible in the experiments conducted with polyA RNA. As an additional control, we confirmed that the reporter protein did not bind to the boxB aptamer when lacking the λN peptide (Fig. S1).

Following this last binding step, a desorption step is included in the assay using buffer B. The biphasic nature of the desorption curves in the experiments conducted with boxBpA and polyA RNAs suggests the presence of some proteins that are non-specifically bound and desorb quickly during the initial steep decay of the signal. However, this is rapidly followed by a much slower decrease. In the case of boxBpA RNA this last signal converges above the initial value, thus confirming that the λN-βLac is stably bound to the boxB aptamer. This is in agreement with the low dissociation constant of this RNA-protein complex reported previously (Austin et al., 2002; Zhang et al., 2010). Stable binding is an important requirement for the biosensor, since the RNA-protein association should be strong enough to withstand the washing steps needed during the test to remove the molecules not hybridized onto the solid support.

The use of two different buffers (A and B) is necessary given the different nature of the molecules involved in the assay. Buffer A is designed to ensure the optimal conditions for RNA refolding (Draper, 2008), however, its composition is not adequate to avoid non-specific RNA/protein interactions given its moderate salt concentration. Therefore, the use of a modified buffer (buffer B) with higher NaCl concentration and incorporating BSA and Tween 20 is necessary. Fig. S2 shows that, indeed, the interaction between λN-βLac and boxBpA (*i.e.* full-length RNA) seems to be stronger when using a salt concentration close to the physiological standard conditions (buffer A). However, a considerable non-specific interaction is detected as well, as can be observed for polyA RNA (lacking the 5' aptamer). Therefore, it is important to minimize this interaction in order to avoid false positives and misinterpretation of the interaction between the different components assayed. The increase in NaCl concentration led to an almost complete removal of the non-specific λN-βLac/polyA interaction. Nevertheless, the λN-βLac/boxBpA interaction decreased as well. This is in agreement with the study of Qi et al. (2010) where the authors report a 10-fold increase in the dissociation constant of the λN/boxB pair, from 2 to 20 nM for monovalent cation concentration of 90 and 220 mM respectively, which are close to those used in buffers A and B. Hence, the increase in the salt concentration in the buffer will decrease the dynamic range and sensitivity of the biosensor. However, this situation is preferred over the conditions leading to non-specific binding, in terms of the design of a functional detection system.

The BLI experiment showed another effect that allowed us to corroborate the specificity of the interaction between boxB and λN-βLac. During the initial seconds of the protein binding, a decreasing signal is observed (Fig. S2b). This effect is attributed to the contraction of the aptamer upon binding with the protein (Bruno, 2015), and is only detectable at the lower NaCl concentration tested, which allows stronger intermolecular interaction. After these few initial seconds the 'positive' contribution to the signal due to the protein binding would mask the 'negative' one corresponding to the RNA contraction. Interestingly, this effect is observed only when boxBpA RNA is loaded on the sensor and not when EV or polyA model RNA are used instead, confirming the previous assumption of the aptamer contraction and the specific nature of this interaction.

In summary, these experiments allowed us to confirm that both binding events required for the correct performance of the biosensor take place selectively only if the relevant ends of the RNA molecule are present. These are the main requirements that the biosensor must fulfil to perform correctly, giving signal only if the assayed RNA molecule is complete and therefore avoiding high baselines and false positives. Additionally, both binding events seemed to take place relatively quickly. More than 90% of the RNA bound during the first 2 min, and most of the λN-βLac protein within a few seconds, features that are important with regards to a final application of the proposed system.

3.3. Biosensor performance tests

The BLI demonstrated that the different components of the biosensor bind as expected and generated a quantifiable output (intensity of RNA and λN peptide binding), but the level of sophistication and the operational costs are not in agreement with the main objective of this work: to keep the complexity of the biosensor as low as possible. Therefore, we aimed to reproduce the conditions of the BLI assay using a simpler platform based on micrometric magnetic beads and nitrocefin. Micrometric beads are a good option for the solid support, since they are easy to handle and suitable for miniaturized applications. Likewise, nitrocefin is a substrate specifically hydrolyzed by β-lactamase with an obvious color change after the reaction, and therefore, suitable as reporter for the assay because it allows both visual determination of the reaction as well as quantitative measurements using spectrophotometry.

3.3.1. Quantitative spectrophotometric analyses

To optimize the biosensor response, the amount of protein needed in the assay and the limit of detection of RNA were studied (Fig. S4). A concentration of 0.6 μM intact RNA was found to be the optimal value, since it was the smallest concentration that lead to the highest biosensor response, thus ensuring linearity in detection as well as a high signal-to-noise ratio.

To analyze the response of the sensor against the degradation extent of the mRNA analyzed, different proportions of boxBpA and polyA (model full length and 5′-end degraded RNAs) were used, fixing the total RNA concentration at 0.6 μM for all the assays. Fig. 4a shows how the signal changes with different amounts of simulated degradation.

The signal from the biosensor is strongly dependent on the proportion of boxBpA RNA present in the assay. Considering the responses for 100% and 0% full-length RNA, the biosensor shows a well-defined ON and OFF state. The high specificity of the λN peptide towards its cognate aptamer as well as the high turnover of β-lactamase (García-García and Draper, 2003; Page, 2008) play an important role in generating the high signal-to-noise ratio observed. In addition, all the intermediate measurements give a response proportional to the concentration of boxBpA. Thus, the results suggest that this system could be suitable for the detection of the integrity of RNA molecules.

Once we confirmed that the sensor showed a response proportional to the integrity of the tested RNA, we proposed two different ways of translating the output, depending on the final application. For industrial and laboratory purposes, where spectrophotometric measurements are available, the interpretation could be based on the rate of nitrocefin hydrolysis. Assuming that the hydrolysis of nitrocefin by λN-βLac takes place following simple Michaelis-Menten kinetics, the product concentration will have a linear correlation with the concentration of enzyme-substrate complex as long as [S]≫[ES] (equation (1)):

$$\frac{d[P]}{dt} = k_2 \cdot [ES] = c; \ \ if \ [S] \gg [E], \tag{1}$$

were [P], [S] and [ES] are the product, substrate and enzyme-substrate concentrations respectively, and k_2 the rate constant for the conversion of ES into E + P. This assumption is equivalent to considering that the concentration of the enzyme-substrate complex is constant, a condition that will be fulfilled during the initial phase of the reaction. Under this circumstance, the initial rate of reaction will only depend on the concentration of [ES], which in the case of the biosensor will be equivalent to the concentration of protein, and therefore of full-length RNA immobilized on the beads. In the particular case of the conditions assayed here, the initial substrate concentration will be more than $2.5 \cdot 10^5$ times higher than the concentration of λN-βLac (taking into account the total amount of protein used in the assay). Thus, it seemed a reasonable assumption to explore if it is possible to generate a linear transfer

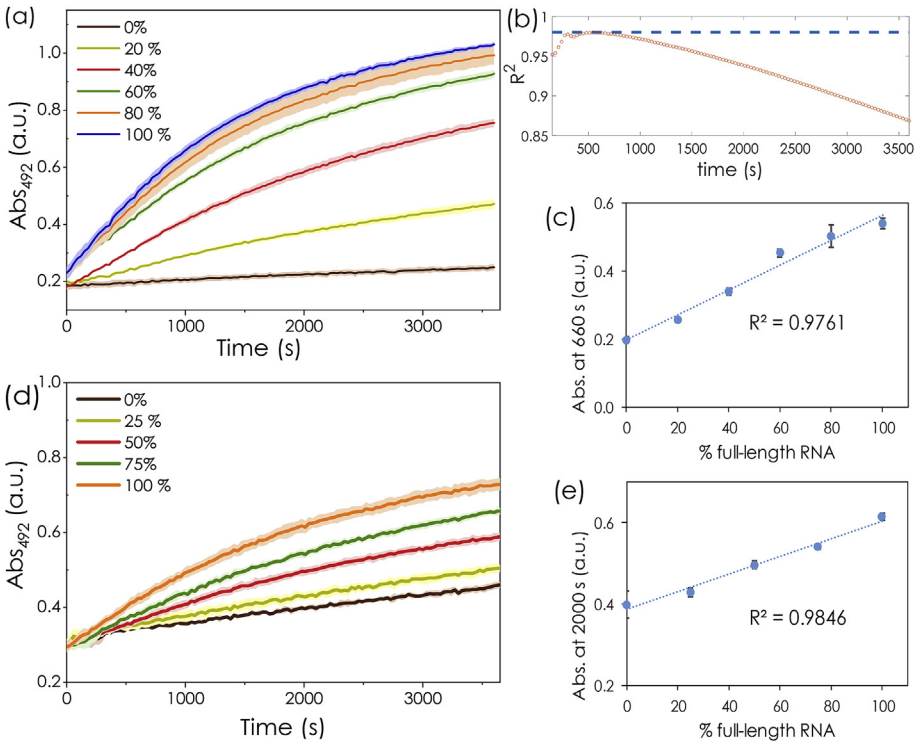

Fig. 4. Biosensor performance. a) Spectroscopic response of the biosensor over time for **different percentages** of **full-length model RNA** (boxBpA). 4 µg of beads were used in each assay, and the absorbance was measured at 492 nm; b) R^2 coefficient obtained from linear fitting of the slopes on (a) for the outputs from t = 0 to t = x, vs time. Horizontal dotted line at $R^2 = 0.975$; c) Transfer function at 660s. The average and SD for three replicate measurements are presented. The results show that the biosensor generates a proportional response with respect to the integrity of the RNA tested, this transfer function being highly linear during the first 10–12 min of assay. d) and e) Performance of the sensor when testing **gene-sized mRNA** (figures equivalent to (a) and (c)). In this case 8 µg of beads were used, and the transfer function was calculated after a longer time (2000 s). When using longer RNAs, the signal of the biosensor is weaker, however under the assayed conditions it maintains its functionality.

function, to enable simple interpretation of the signal.

Fig. 4b shows the R^2 coefficient obtained from the linear fitting of the absorbance increase considering the points from t = 0 to t = x (thus resembling the initial reaction rate during the first moments of the reaction), versus time. The obtained data show that the assumption of a constant reaction rate holds during the first 10–12 min of reaction for all the condition assayed, with $R^2 \geq 0.975$. This linear correlation is lost once the concentration of substrate is substantially depleted. Given the design of the biosensor, only one λN-βLac molecule can be attached to each RNA molecule. Consequently, within this period of time, the amount of hydrolyzed nitrocefin will be linearly related to the amount of λN-βLac, and by extension, to the amount of full-length RNA. Therefore, the biosensor is able to effectively correlate the percentage of full-length RNA with the absorbance within the linear range of its transfer function, as shown in Fig. 4c, where it is calculated at 660 s.

The performance of the sensor was also tested with mRNAs of a size similar to the average gene-encoding molecule. Fig. 4c and d shows the results of the assay conducted with pA-lac and boxBpA-lac mRNAs. Similar to the results for the shorter model RNA molecules, a linear transfer function was obtained, enabling the quantification of the amount of full-length mRNA (boxBpA-lac in this case). However, it is important to note the slower response and smaller dynamic range, which can be explained by a decrease in efficiency in the recognition of the boxB aptamer by the λN peptide with an increase in the RNA length, caused by the more complex 3D structure of the molecule. Biolayer interferometry corroborated this explanation (Fig. S3). The steeper baseline (corresponding to 0% full-length RNA) indicates the occurrence of non-specific electrostatic RNA/protein interactions, that would be more likely in longer RNA molecules. These results suggest that the future development of an optimized 5' region with a reduced tertiary structure would boost the response of the sensor, especially for longer RNAs. This would take advantage of the design of the proposed detection system, which only relies on the nucleotides on the ends of the molecule, which will be more accessible even when complex structures occur internally.

In section 4.2, the importance of optimizing salt concentration to decrease non-specific binding was demonstrated. As an example, Fig. S5 shows the performance of the biosensor when using only buffer A throughout all the steps. The existence of non-specific interactions between polyA RNA and the protein considerably reduced the sensitivity of the sensor. It is also important to note that using magnetic beads means the need for a centrifuge can be circumvented, in line with the aim of developing a biosensor suitable for field applications. In addition, it can increase the accuracy of the assay by minimizing the loss of material compared to other similar beads like silica (Fig. S6).

3.3.2. *Visual detection analyses*

The second proposed approach makes use of the simplicity of the biosensor, which is suitable for end-user applications where specialized equipment is not available. Here we propose a visual test, where a sample of beads and nitrocefin reaction mix are loaded on to a hydrophobic surface (e.g. parafilm) with a colored background. By a simple visual comparison, it is possible to estimate the amount of full-length RNA. As shown in Fig. 5 and Supplementary Video 1, the red background dots disappear at distinctly different time points depending on the amount of full-length RNA used in the binding assays. As can been observed, the background dot disappears after 17.3 min for 100% full-length RNA. Thus, a calibrated background reference will allow the estimation of the integrity of the RNA tested.

Supplementary video related to this article can be found at https://doi.org/10.1016/j.bios.2019.05.008.

Consequently, the proposed biosensor is reliable enough to be used in analysis of RNA, being capable of detecting shifts in the integrity of mRNAs with less than 35 ng of analyte, an amount comparable to that required for microfluidic electrophoresis, the standard RNA quantification and characterization technique (e.g. the Agilent Bioanalyzer system has a limit of detection above 25 ng). Given the specificity of the sensor towards both ends of the RNA molecule, it would also find applications in detecting incomplete transcripts and preliminary RNA degradation. In addition, the simplicity of the approach would allow the use of the biosensor, for example, during on-field vaccination campaigns where no technical equipment is available. This is an important issue to address for this kind of vaccine if they are to ultimately succeed as an alternative and low cost prophylaxis strategy (Kis et al.,

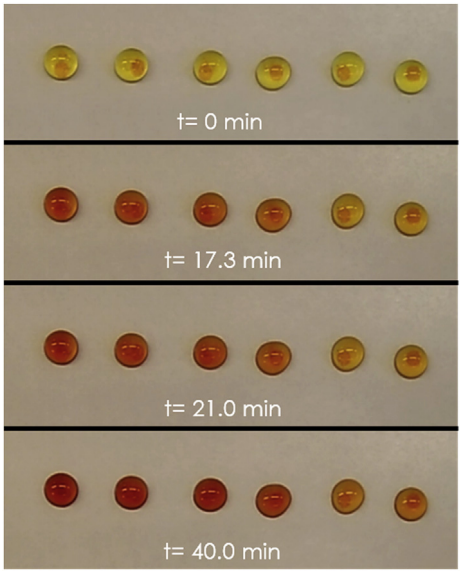

Fig. 5. Visual response of the biosensor over time for different percentages of full-length RNA (boxBpA). 1 μg of magnetic beads resulting from the integrity assay were loaded on top of the red-background dot paper (coated with parafilm) and then 19 μL reaction mix (with nitrocefin at 30%) were added (time = 0). From left to right the different samples correspond to: 100%, 80%, 60%, 40%, 20% and 0% of boxBpA RNA used in the integrity assay. It can be observed that the background is no longer visible after 17.3 min for 100% and 21 min for 80% of full-length RNA. (For interpretation of the references to color in this figure legend, the reader is referred to the Web version of this article.)

2019; Sahin et al., 2014).

To the best of our knowledge, this is the first reported biosensor to measure mRNA integrity that does not require specialized equipment. However, it is also important to note that the mechanism of the sensor requires the incorporation of an aptamer in the 5′-end. Although it has been reported that these structures present low immogenicity (Alsaafin and McKeague, 2017), optimization may be required to ensure the presence of the aptamer in the 5′ UTR is not disruptive for the mRNA function. In addition, there could be non-specific binding between the RNA-binding peptide and the mRNA, the probability of which increases for longer transcripts. However, this issue could be surpassed by using highly specific RNA-binding peptide/aptamer pairs such as λN/boxB (Lampasona and Czaplinski, 2016), and enhancing their affinity and specificity through rational design or directed evolution (Austin et al., 2002; Qi et al., 2010).

4. Conclusions

In this work we developed a biosensor designed to test the integrity of an RNA molecule with simplicity and on-field applicability in mind. A recombinant fusion protein, λN-βLac, is the main component of the biosensor and has two functions: (i) specific recognition of a hairpin (boxB), and (ii) transduction of the signal. The mechanism of action of the biosensor is based on the presence of a hairpin (boxB) and a polyA tail at the 5′ and 3′ ends of the RNA molecule to be tested. Additionally, the sensor relies on a polydT-functionalized support where the RNA is retained by its polyA tail. In this work we have shown that all the components of the biosensor bind as desired, allowing a response only if the RNA molecule is complete. We have been able to minimize problems derived from non-specific binding by varying the concentration of salt and molecular crowding agents. More significantly, we have demonstrated that the designed biosensor shows a linear response against the integrity of the tested RNA. This feature enables a simple interpretation of the transfer function. We have also shown that this system is applicable to gene-length mRNAs. Therefore, the biosensor would be applicable for on-field uses, requiring only a visual test to estimate the integrity of an RNA molecule. In addition, because of its specificity towards both RNA ends and accuracy of response, it could be of interest for routine industrial quality control analyses or more sophisticated laboratory uses that already require polyA-based RNA purification such as transcriptome studies. This test could be easily incorporated in the workflow with a small aliquot of the purified RNA.

Data statement

All data not included in the manuscript are available upon request from the corresponding author and can be used without restriction.

Declaration of interests

☒ The authors declare that they have no known competing financial interests or personal relationships that could have appeared to influence the work reported in this paper.

☐The authors declare the following financial interests/personal relationships which may be considered as potential competing interests:

CRediT authorship contribution statement

Ignacio Moya Ramírez: Conceptualization, Formal analysis, Investigation, Methodology, Writing - original draft, Writing - review & editing. **Cleo Kontoravdi:** Conceptualization, Funding acquisition, Project administration, Writing - review & editing. **Karen M. Polizzi:** Conceptualization, Funding acquisition, Project administration, Writing - review & editing.

Acknowledgments

The authors acknowledge the EPSRC (project EP/K038648/1) for funding this work. The authors acknowledge Pascale Legault for kindly making the plasmid pET42a-λN + -L + -GSH available.

Appendix A. Supplementary data

Supplementary data to this article can be found online at https://doi.org/10.1016/j.bios.2019.05.008.

References

Alsaafin, A., McKeague, M., 2017. Biosens. Bioelectron. 94, 94–106.
Austin, R.J., Xia, T., Ren, J., Takahashi, T.T., Roberts, R.W., 2002. J. Am. Chem. Soc. 124, 10966–10967.
Blewett, N., Coller, J., Goldstrohm, A., 2011. RNA 17, 535–543.
Bruno, J.G., 2015. Molecules 20, 6866–6887.
Cantara, W.A., Hatterschide, J., Wu, W., Musier-Forsyth, K., 2017. RNA 23, 240–249.
Carlson, R., 2016. Nat. Biotechnol. 34, 247–255.
Carrascosa, L.G., Gómez-Montes, S., Aviñó, A., Nadal, A., Pla, M., Eritja, R., Lechuga, L.M., 2012. Nucleic Acids Res. 40, 8.
Carrascosa, L.G., Huertas, C.S., Lechuga, L.M., 2016. Trends Anal. Chem. 80, 177–189.
Choi, J., Seong, T.W., Jeun, M., Lee, K.H., 2017. Adv. Healthc. Mater. 6 (1700796), 1–14.
Constantinou, A., Polizzi, K.M., 2013. Biochem. Soc. Trans. 41, 1146–1151.
Daigle, N., Ellenberg, J., 2007. Nat. Methods 4, 633–636.
Di Tomasso, G., Lampron, P., Dagenais, P., Omichinski, J.G., Legault, P., 2011. Nucleic Acids Res. 39, 3.
Draper, D.E., 2008. Biophys. J. 95, 5489–5495.
Fang, S., Lee, H.J., Wark, A.W., Corn, R.M., 2006. J. Am. Chem. Soc. 128, 14044–14046.
García-García, C., Draper, D.E., 2003. J. Mol. Biol. 331, 75–88.
Gibson, D., Young, L., Chuang, R., Venter, J., Hutchison, C., Smith, H., 2009. Nat. Methods 6, 343–345.
Halford, C., Gau, V., Churchill, B.M., Haake, D.A., 2013. J. Vis. Exp. 74, 1–8.
Hall, E.A.H., Chen, S., Chun, J., Du, Y., Zhao, Z., 2016. Trends Anal. Chem. 79, 247–256.
Hu, J., Wang, S.Q., Wang, L., Li, F., Pingguan-Murphy, B., Lu, T.J., Xu, F., 2014. Biosens. Bioelectron. 54, 585–597.
Kawakami, J., Sugimoto, N., Tokitoh, H., Tanabe, Y., 2006. Nucleos Nucleot. Nucleic Acids 25, 397–416.
Ke, W., Laurent, A.H., Armstrong, M.D., Chen, Y., Smith, W.E., Liang, J., Wright, C.M., Ostermeier, M., van den Akker, F., 2012. PLoS One 7, 6.
Kis, Z., Shattock, R., Shah, N., Kontoravdi, C., 2019. Biotechnol. J. 14, 1800376.

La Manno, G., Soldatov, R., Zeisel, A., Braun, E., Hochgerner, H., Petukhov, V., Lidschreiber, K., Kastriti, M.E., Lönnerberg, P., Furlan, A., Fan, J., Borm, L.E., Liu, Z., van Bruggen, D., Guo, J., He, X., Barker, R., Sundström, E., Castelo-Branco, G., Cramer, P., Adameyko, I., Linnarsson, S., Kharchenko, P.V., 2018. Nature 560, 494–498.
Lampasona, A.A., Czaplinski, K., 2016. Methods 98, 10–17.
Martin, R.M., Rino, J., Carvalho, C., Kirchhausen, T., Carmo-Fonseca, M., 2013. Cell Rep. 4, 1144–1155.
Mishra, S., Mohan, S., Godavarthi, S., Sen, R., 2013. J. Biol. Chem. 288, 28089–28103.
Morrison, C., Lähteenmäki, R., 2018. Nat. Biotechnol. 36, 576–584.
Page, M.G.P., 2008. Clin. Microbiol. Infect. 14, 63–74.
Pardi, N., Hogan, M.J., Porter, F.W., Weissman, D., 2018. Nat. Rev. Drug Discov. 17, 261–279.
Philp, J., 2018. N. Biotech. 40, 11–19.
Polizzi, K.M., Kontoravdi, C., 2015. Curr. Opin. Biotechnol. 31, 50–56.
Qi, X., Xia, T., Roberts, R.W., 2010. Biochemistry 49, 5782–5789.
Sahin, U., Karikó, K., Türeci, Ö., 2014. Nat. Rev. Drug Discov. 13, 759–780.
Santangelo, T.J., Artsimovitch, I., 2011. Nat. Rev. Microbiol. 9, 319–329.
Strobel, E.J., Yu, A.M., Lucks, J.B., 2018. Nat. Rev. Genet. 19, 615–634.
Tan, R., Frankel, A.D., 1995. Proc. Natl. Acad. Sci. 92, 5282–5286.
Tedeschi, L., Citti, L., Domenici, C., 2005. Biosens. Bioelectron. 20, 2376–2385.
Vigneshvar, S., Sudhakumari, C., Senthilkumaran, B., Prakash, H., 2016. Front. Bioeng. Biotechnol. 4, 1–9.
Zhang, X., Lee, S.W., Zhao, L., Xia, T., Qin, P.Z., 2010. RNA 16, 2474–2483.
Zhang, A., Sun, H., Xu, H., Qiu, S., Wang, X., 2013. Cell metabolomics. Omi. A J. Integr. Biol. 17, 495–501.